





# Physico-Chemical Characterization of Historic Mortars from the Venetian Arsenals of Chania (Greece)

Pagona-Noni Maravelaki<sup>(✉)</sup> , Kali Kapetanaki ,  
and Nikolaos Kallithrakas-Kontos 

Technical University of Crete, 73100 Chania, Greece  
pmaravelaki@tuc.gr

**Abstract.** The Venetian Arsenals of Chania in southern Greece constitute an important monument of cultural and industrial heritage, as well as a key landmark for the town. In the framework of the holistic study for the restoration of the building, mortars, plasters, and stones were sampled and analyzed in order to identify the construction phases and evaluate the decay state of the materials. Open porosity, bulk density and soluble salts were measured. Additionally, the mortars were chemically and mineralogically characterized through X-ray fluorescence analysis (XRF), infrared spectroscopy (FTIR), differential thermogravimetric analysis (DTA/TG) and X-Ray diffraction (XRD) to identify the mortars' technology and the composition of the raw materials. Furthermore, the granulometric analysis and the optical microscopy provided information about the aggregates and the consistency of the mortars. The original Venetian mortars exhibited good consistency and excellent coherence with the building stones. The Ottoman mortars, on the contrary, due to their poor consistency, have suffered the greatest decay. This research constitutes the base for the design of compatible restoration materials, thus ensuring the sustainable performance of the monument.

**Keywords:** mortars · characterization · binder · aggregates · construction phases

## 1 Introduction

The construction of the Chania Arsenals began in 1497 and gradually the addition of two impressive complexes were eventually formed. The first, at the eastern end of the harbor, comprised five Arsenals, while the other, further east, alongside today's dock, which had not been constructed at that time, consisted of seventeen adjacent Arsenals.

The dome sheds of the Arsenals, which had finial pediment facades open to the sea for the approaching ships, were almost 50 m long, 9 m wide, with an average height of 10 m. Arched passageways completed the transverse walls. The Arsenals were constructed of ashlar sandstone in the perimeters of the arches and the walls consisted of rubble stones. By the end of the 19th century the seventeen-arsenals complex had only seven remaining domes (see Fig. 1). In the beginning of the 20th century, the open sea front arches were sealed with walls, the dock was constructed, and the area changed radically. Over the

years, the Arsenals had various uses such as storage, laboratories of Archaeological services, venue for events and exhibitions. Nowadays, due to the plethora of decay issues they are only used as storage [1].

In the framework of a research project of the Technical University of Crete entitled “Investigation of the historical and technological documentation and the proposal of new uses – promotion of the Arsenals in Chania”, historical materials such as, mortars, plasters and stones were sampled and analyzed. More than 35 samples of mortars and plasters were extracted and analyzed in order to identify their composition, consistency, as well as their current condition.

The analysis and characterization of the original materials of historical structures constitutes a helpful tool for the determination of the construction phases, the current condition, and the design of restoration mortars [2–4]. Therefore, the physico-chemical and mineralogical characterization of the raw materials and the derived historical mortars provided information about the Arsenals’ construction phases, namely the initial Venetian, the Ottoman, and modern interventions. According to the analyses carried out three main groups of original historical mortars and plasters were identified; the 1st group consists of air lime mortars, the 2nd one of moderately hydraulic mortars and the 3rd one of hydraulic mortars.



**Fig. 1.** Panoramic view of the seven Arsenals of Chania.

## 2 Experimental Part

### 2.1 Sampling

The samples were extracted in a gentle way without causing any destruction to the monument, trying to cover various parameters such as the interior or exterior exposure, orientation, and origin, i.e. Venetian, Ottoman or newer. The sampling positions are illustrated in Fig. 2. The samples labeled according to the following coding system:

$$N [1] [2] [3] [4] - I \quad (1)$$

where, N: First letter, used for every sample; 1: labeled as (a), (b) or (c) depending on the construction phase of Arsenal, Venetian, Ottoman, newer, respectively; 2: Filled from 1 to 7, depending on the serial number of Arsenal, starting from west to east; 3: labeled as (i) for samples from internal and as (e) for samples from external exposure sides; 4: labeled as j: for joint mortars, as r: for rubble masonry mortars and as pl: for plasters; I: the serial number of the sample.

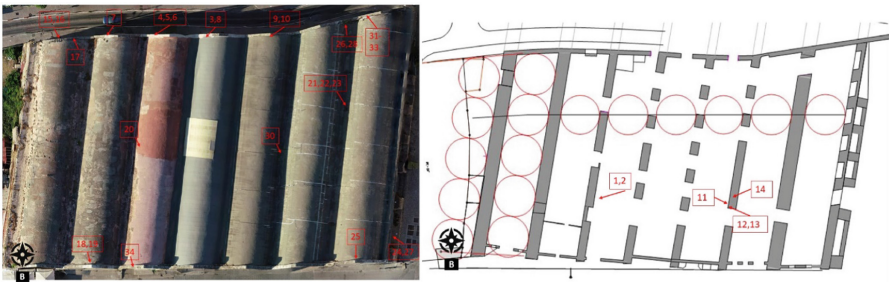


**Fig. 2.** Sampling location: view of vaults of the Arsenals and external sampling points (left) and plan of the ground floor with indication of the internal sampling points (right).

### 2.2 Methods for the Characterization of the Samples

Firstly, the original mortar samples were macroscopically observed and divided into 3 groups according to their color; the 1st group consists of the white ones, the 2nd of the grey ones and the 3rd contains the red samples.

Afterwards, the microstructure of the samples was observed using the digital optical microscope USB Dino-Lite AM4515T5 Edge with a color CMOS sensor. The apparent density, the absorbed humidity and the open porosity were also measured after immersion of desiccated samples into water for 2 days at least. Following, the grain size distribution was carried out by mechanical sieving (ASTM E 11-70 series of sieves, meshes of 4.5, 2, 1, 0.5, 0.25, 0.125 and 0.063 mm of diameter) in order to separate the binder from the aggregates and implement the grain size distribution analysis. This destructive method required a large quantity of samples and for that reason only 3 samples of each group were analyzed.

The chemical and mineralogical characterization were carried out through FTIR, XRF and X-ray diffraction (XRD) analyses, respectively. The XRF instrumentation included  $^{109}\text{Cd}$  and  $^{55}\text{Fe}$  radioactive sources and a Si(Li) semiconductor detector, and the FTIR analysis was carried out with a Thermo Scientific Nicolet<sup>TM</sup> iS50 FT-IR device. Mineralogical composition was assessed with XRD on a Bruker D8 Advance Diffractometer, using Ni-filtered Cu K radiation (35 kV 35 mA) and a Bruker Lynx Eye strip silicon detector, in  $40\text{--}70^\circ$  2-theta range, with  $0.02^\circ$  step size and 0.2 s per step. Additionally, DTA-TG analyses were carried out to further evaluate the existence of hydraulic compounds, using a Setaram LabSys Evo 1600 °C thermal analyzer up to 1000 °C under nitrogen atmosphere with a heating rate of 10 °C/min at a flow rate of 30 mL/min in aluminum crucible.

Finally, the amount of salts present in the historical mortars was estimated through conductivity measurements [5], using a GLP31 Crison conductometer. More specifically, 0.1 g of the binder is dissolved in 100 mL water and remains under magnetic stirring for 2 days. Afterwards, the conductivity of the sol is measured (ES). The salt content (TDS) is calculated according to the Eq. 2:

$$\text{TDS}(\text{mg/L}) = 0.068 * \text{ES}(\mu\text{S/cm}) \quad (2)$$

## 3 Results

### 3.1 Macroscopic and Stereoscopic Analysis

The macroscopic and stereoscopic observation of the 1<sup>st</sup> group of white samples, illustrated in Fig. 3, revealed a moderate [sample (b) Nb3ep-8] to good [sample (a) Nb4er-4] consistency and proper mixing. However, in some cases salt deposits as well as small cracks were also observed [sample (d) Nb6er-19]. The size of aggregates varies, but it does not exceed the diameter of 4 mm.

The 2<sup>nd</sup> group of grey samples exhibited a poor consistency macroscopically as they were brittle, in accordance with the optical microscopy observations that revealed small cracks and large pores on their surface (Fig. 4). The size of aggregates was varied, exhibiting a diameter lower than 4 mm.

The sample Na1er-33-3 is a typical example of the layered mortar that protected the external part of vaults and consisted of the internal rubble mortar layer (b and d) the intermediate layer (c) and the external thin plaster. All three layers have a good consistency, and their different color could be attributed to the addition of soil material to the rubble mortar and external plaster (Fig. 5 d). Additionally, the rubble mortar also consisted of large aggregates (Fig. 5 b), whilst agglomerations of lime are observed in the internal and intermediate layers even with the naked eye.

The red group of mortars has Ottoman origin, since the samples have been selected from areas attributed to interventions during the Ottoman period (Fig. 6). The samples consisted of soil material and lime and small aggregates. Small cracks and pores are observed along with agglomerations of lime. The consistency is poor, and the mortars are too brittle. All the aggregates have a rounded shape, denoting the use of river sand.

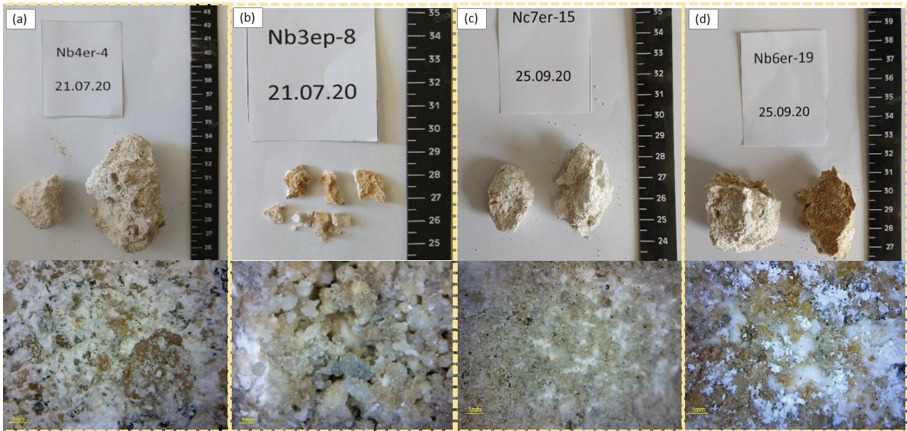


**Fig. 3.** Macroscopic and optical microscopic inspection of the 1<sup>st</sup> group of white mortar samples: (a) Sample Nb4er-4; (b) Sample Nb3ep-8; (c) Sample Nc7er-15; (d) Sample Nb6er-19.

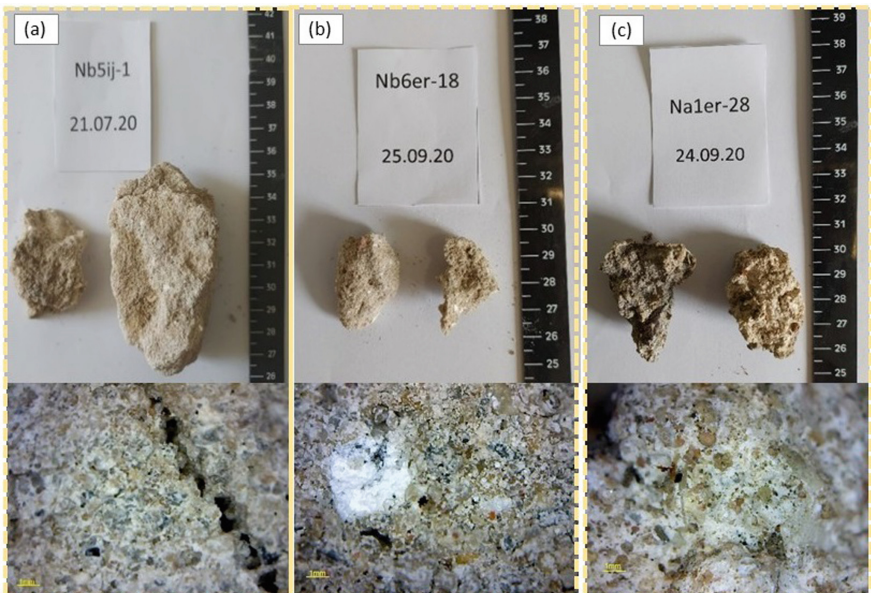


**Fig. 4.** Macroscopic and optical microscopic inspection of the 2<sup>nd</sup> group of grey mortar samples: (a) Sample Nb5ij-1; (b) Sample Nb6er-18-8; (c) Sample Na1er-28.

### 3.2 Grain Size Distribution and Physical Properties of Samples

The apparent density, the wt. % absorbed humidity, the open porosity (%) as well as the wt. % of soluble salts of the tested samples are listed in Table 1. All samples seem to have similar values concerning the accessible porosity and the apparent density. The sample Nb3er-10, mostly consisting of soil, exhibited the highest wt. % of humidity along with

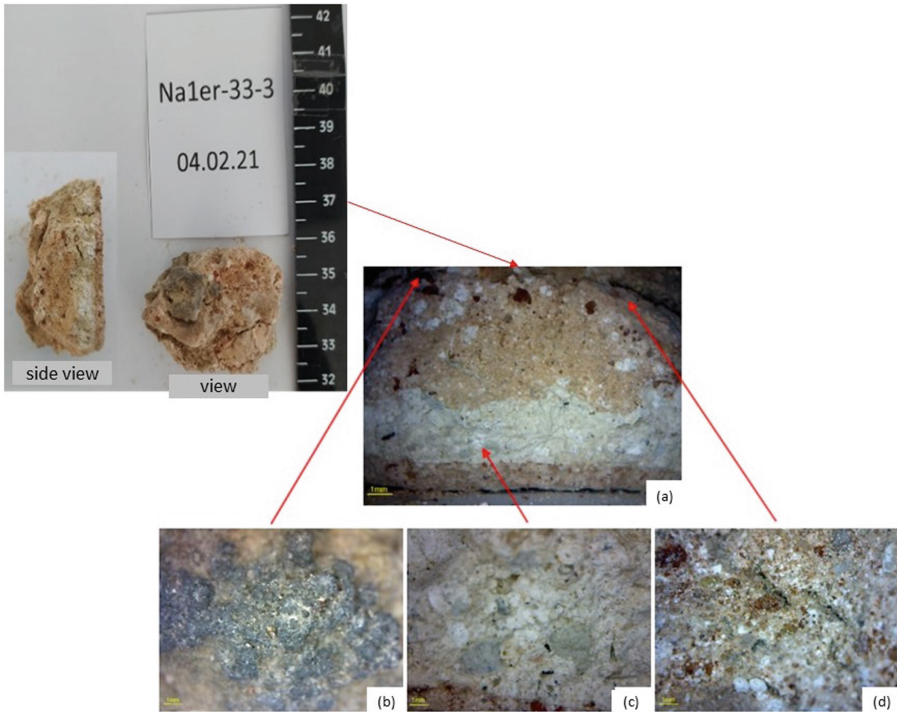


**Fig. 5.** Macroscopic and optical microscopic inspection of the 3-layered mortar Na1er-33-3 on the external part of vaults.

a large porosity and density, whereas the mortar Nb4er-4 has the lowest porosity, a fact that could be attributed to the good consistency and lack of cracks.

The presence of salts was quite evident in the macroscopic and microscopic observation of the samples, especially in brittle samples, where salts deposits were noted. The wt. % content of salts is higher in the rubble mortars, as they are located inside the masonry suffering from trapped moisture. The high salt content is expected, due to the proximity of the monument to the sea.

The grain size distribution of samples Nb5ij-1 (grey), Nb4er-4 (white) and Nc7er-16 (red-ottoman) was compared to the curve of standard sand in Fig. 7. It was revealed that all three tested samples have coarser aggregates compared to the grain size distribution of the standard sand's. It should be emphasized that the granulometric curve of the Nb4er-4 sample, which has a Venetian origin, is close to the standard sand's curve exhibiting a proper sigmoid grain size distribution along with good consistency, as mentioned above. On the contrary, the sample Nc7er-16 has the most heterogeneous distribution as most of the aggregates range in the zone of 15–25 mm in diameter.

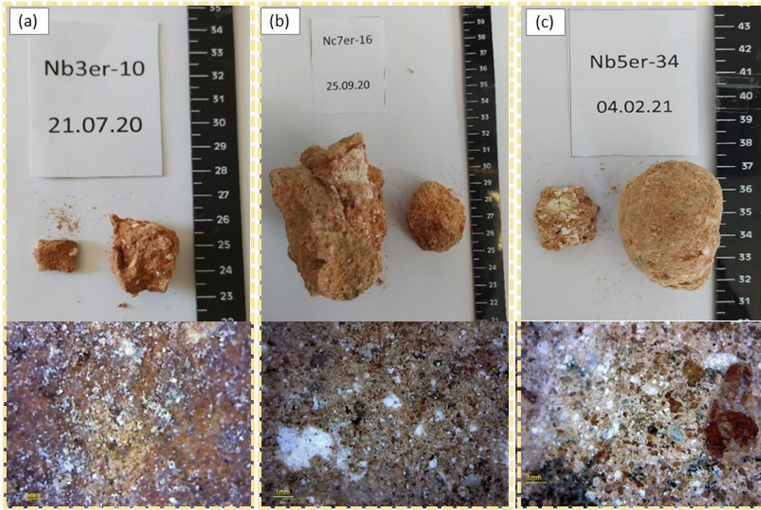


**Fig. 6.** Macroscopic and optical microscopic inspection of the 3<sup>rd</sup> group of red mortar samples: (a) Sample Nb3er-10; (b) Sample Nc7er-16; (c) Sample Nb5er-34.

**Table 1.** Characteristics of samples

Sample	Humidity (wt. %)	Open Porosity (%)	Apparent Density (g/mL)	Soluble Salts (wt. %)
Nb5ij-1	0.31	27.4	2.43	1.98
Nb4er-4	0.99	20.7	2.53	3.89
Nc7er-15	2.64	29.6	2.13	4.48
Nb3er-10	5.05	31.0	2.33	9.40

### 3.3 FTIR, XRF and DTA Analyses

The XRF results illustrated in Fig. 8, revealed calcium as the predominant element in the white samples (Nb4er-4 and Nb4er-15), along with silicon, iron, magnesium, sodium, and aluminum in lower proportions concentrations. The grey sample Nb5ij-1 differs slightly from the white samples, as silicon's concentration is higher, a fact that could be related to the presence of hydraulic compounds. Concerning the Ottoman sample Nb3er-10, although it has a high amount of calcium, it also contains a high percentage of silicon, aluminum, iron and magnesium. This finding could be attributed to the presence of soil material and/or the deliberate addition of ceramic crust, a methodology which was very common to Ottomans. Finally, all rubble mortars contain considerable amounts of sodium and chloride due to the presence of sea salts deposits.

The presence of hydraulic compound in the mortar samples was further evaluated though FTIR and DTA/TG analyses.

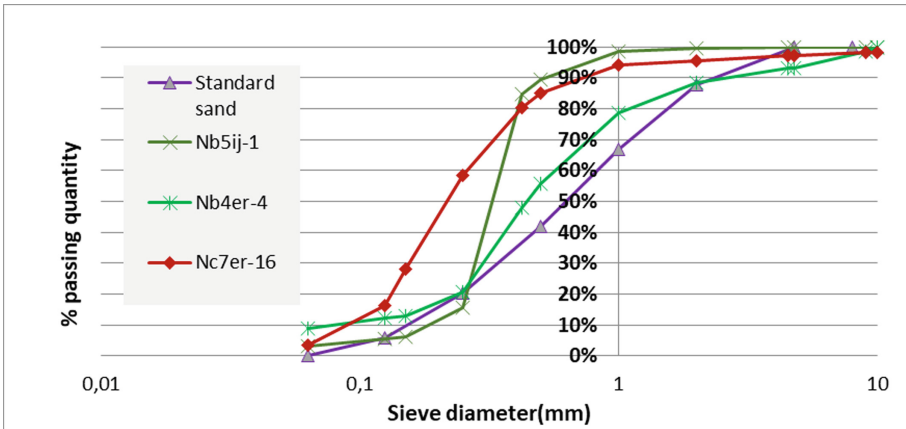


Fig. 7. Granulometric curves of the mortars' aggregates and comparison to the standard sand's.

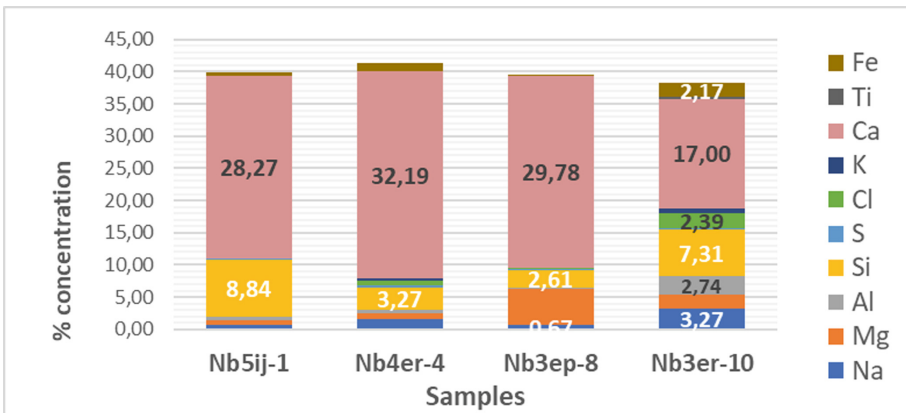


Fig. 8. Elemental composition of samples according to the XRF analysis.

Three samples of each group were analysed through DTA/TG (see Fig. 9). The endothermic reaction between 600–900 °C indicates the decomposition of calcium carbonate (Cc). Moreover, the endothermic reaction along with the corresponding mass loss around 100 °C, expresses the dehydration of the bound water of each, whilst the reaction around 400 °C shows the dehydroxylation of the hydraulic components [6, 7]. As revealed in Fig. 9, the samples of Venetian origin Nb4er-4 (a) and Nb6er-18 (b) exhibit a high percentage of calcium carbonate, whereas the sample Nc7er-16 (c) belonging to the Ottoman period shows a considerable amount of aluminosilicate components, originating from the addition of ceramic crust and soil material.

Calculating the mass losses during the endothermic reaction between 600–900 °C (ML) and considering the molar mass (MM) of calcium carbonate and carbon dioxide, the percentage of calcium carbonate (Cc) can be determined. The Venetian origin samples



Nb4er-4 and Nb6er-18 show a Cc content (wt. %) of 65.51 and 60.02, respectively, whereas in the Ottoman origin sample Nc7er-16 the Cc wt. % content is equal to 29.71.

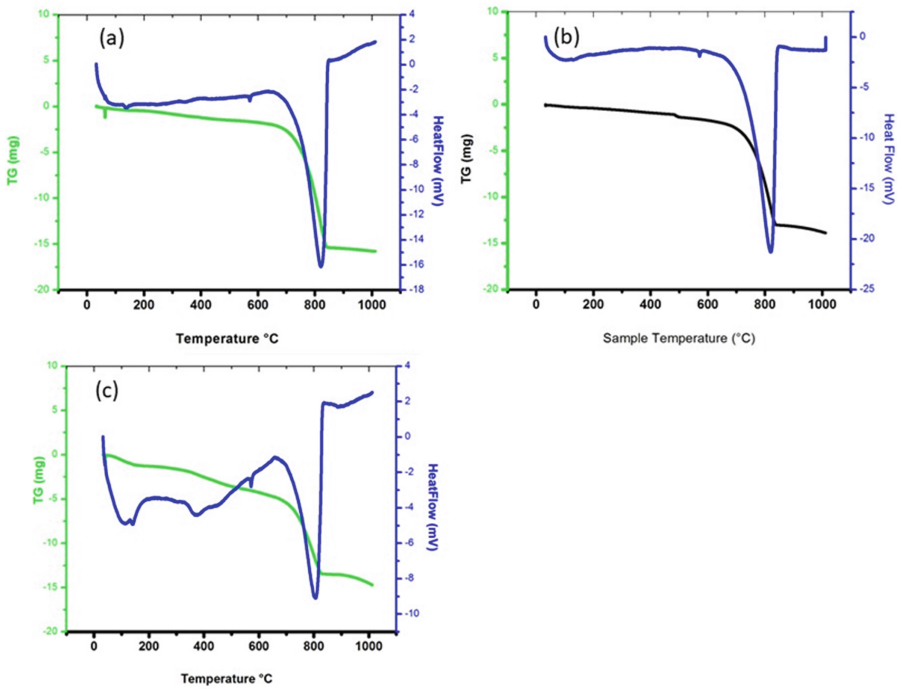


**Fig. 9.** DTA/TG analysis for samples of Venetian origin Nb4er-4 (a) and Nb6er-18 (b), and the Ottoman origin sample Nc7er-16 (c).

The FTIR spectra of samples are illustrated in Figs. 10–12. The predominant peaks are attributed to calcium carbonate ( $1440$ ,  $870$  and  $712\text{ cm}^{-1}$ ). Additionally, the absorptions around  $1100$ – $1030$ ,  $780$  and  $460\text{ cm}^{-1}$  are associated with silicon oxygen bond vibrations (Si-O-Si and Si-O) [8]. More specifically, the peaks in the range  $900$ – $1000\text{ cm}^{-1}$  are attributed to hydraulic components, with the peak at  $900\text{ cm}^{-1}$  to be indicative of the hydraulic lime, whereas the peak at  $780\text{ cm}^{-1}$  is attributed to quartz [8–10]. Moreover, the intense peak at  $1385\text{ cm}^{-1}$  of sample Nb4er-4 (Fig. 10, a) is assigned to nitrogen-oxygen (N-O) bond vibrations, due to the presence of nitrate ions and in particular  $\text{KNO}_3$ . The presence of nitrates is associated with agricultural activities through which they penetrate the aquifer. Finally, the FTIR spectra of aggregates reported in Fig. 13 showed that both carbonaceous and siliceous sand were used, depending on the origin of the river.

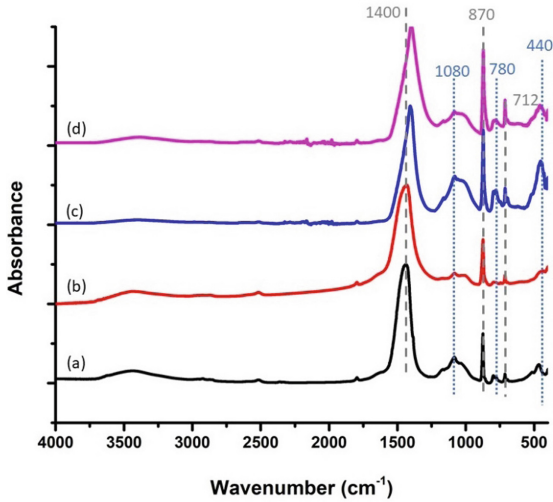


**Fig. 10.** FTIR spectra of the 1<sup>st</sup> group white samples; (a) Nb4er-4; (b) Nb3ep-8; (c) Nc7er15; (d) Nb6er-19.

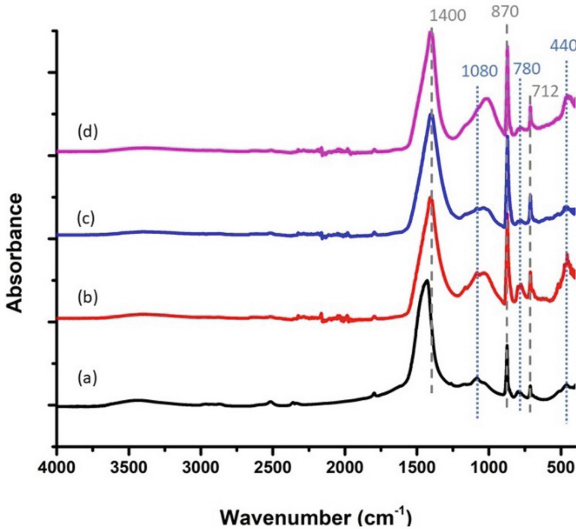


**Fig. 11.** FTIR spectra of the 2<sup>nd</sup> group of grey samples; (a) Nb5ij-1; (b) Nb6er-18; (c) Na1er-28; (d) Na1er-33-2.

### 3.4 Mineralogical Analysis

The results of the XRD analysis depicted in the x-ray diffractograms on Fig. 14, showed that the predominant mineral in the mortars was calcite (Calcite, Cc) followed by quartz (Quartz, Qz). The red Ottoman period Nb3er-10 sample, has a high content of quartz

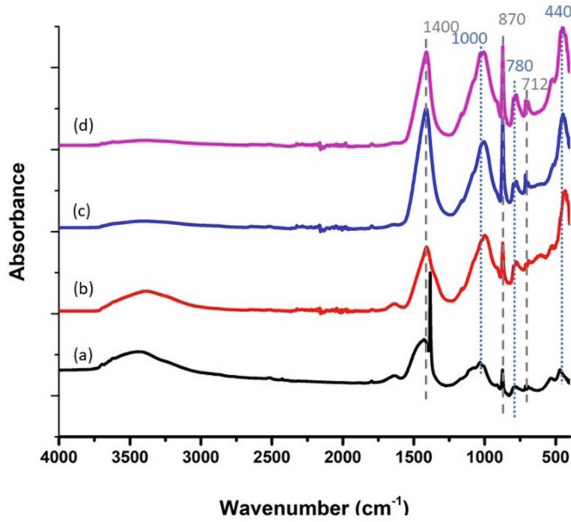


**Fig. 12.** FTIR spectra of the 3<sup>rd</sup> group of the red samples; (a) Nb3er-10; (b) Nc7er-16; (c) Nb5er-34; (d) Na1er-33-3 (inside layer).

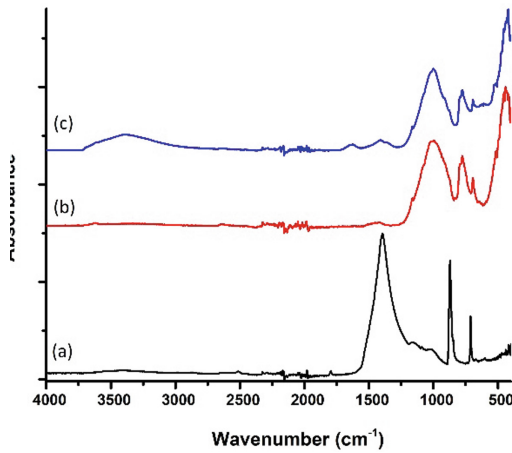


**Fig. 13.** FTIR spectra of the aggregates of samples: grey, Nb6er-18 (a); white, Nc7er15 (b); red, Nc7er-16 (c).

due to added ceramic material. In addition, Halite (HI) was found in low quantity, due to sea salts [11]. Finally, the low addition of soil material was ascertained by the existence of Kaolinite (KI).

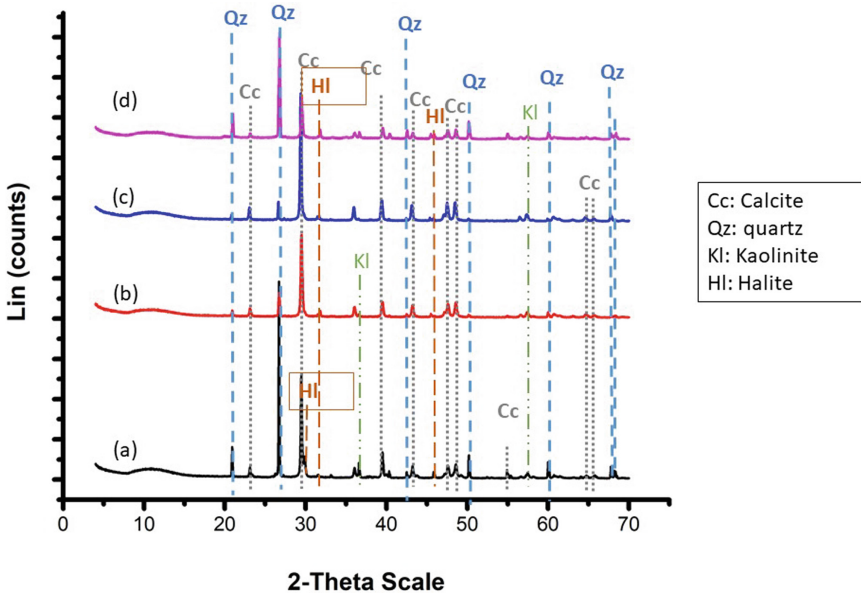


**Fig. 14.** XRD pattern of the samples: grey, (a) Nb5ij-1; white, (b) Nb4er-4; white, (c) Nc7er-15; red, (d) Nb3er-10.

## 4 Conclusions

Summarizing the above observations, it could be concluded that:

- The examined samples are quite porous lime-based mortars with moderate consistency due to decay from environmental factors, such as sea aerosol, humidity, intense winds, and water capillarity absorption. All samples show nitrate and chloride attack, as evidenced by FTIR, XRF and conductivity measurements.
- FTIR and XRD analyses indicated the presence of aluminosilicates and magnesium compounds, apart from calcium carbonate, in a smaller percentage, a fact that can be attributed to the use of soil material and ceramics of different gradation during the composition of mortars.
- According to the results of the grain size distribution, only the original Venetian mortars have a proper sigmoidal distribution of aggregates. The aggregates are both of calcareous and siliceous nature with round grains, so they originated from river sand.
- There is a differentiation of mortars by the degree of hydraulicity, which is attributed to the use of moderate hydraulic lime manufactured from the firing of marly limestones found in the area, but also to the use of artificial pozzolans, such as fragments of fine-grained or crushed ceramic.
- The use of hydraulic lime could be assigned to Venetian technology, whereas the high addition of fine-grained ceramic powder belongs to the Ottoman technology, as assumed by the constructions' phases.

- The Venetian mortars, despite the decay they suffered, show better cohesion than the Ottomans which are brittle.

The above conclusions can lead to an effective design of repair mortars, compatible to the original Venetian ones with enhanced durability.

## References

1. Lane, F.C.: Venice, A Maritime Republic. Johns Hopkins University Press, ISBN 978-0801814600 (1973)
2. Maravelaki, P.N., Theologitis, A., Budak Unaler, M., Kapridaki, C., Kapetanaki, K., Wright, J.: Characterization of Ancient Mortars from Minoan City of Kommos in Crete. *Heritage* **4**(4), 3908–3918 (2021). <https://doi.org/10.3390/heritage4040214>
3. Stefanidou, M., Pachta, V., Konopissi, S., Karkadelidou, F., Papayianni, I.: Analysis and characterization of hydraulic mortars from ancient cisterns and baths in Greece. *Mater. Struct.* **47**(4), 571–580 (2013). <https://doi.org/10.1617/s11527-013-0080-y>
4. Velosa, A.L., Veiga, R., Coroado, J., Ferreira, V.M., Rocha, F.: Characterization of ancient Pozzolanic mortars from Roman times to the 19th century: compatibility issues of new mortars with substrates and ancient mortars. In: Dan M.B., Příkryl R., Török Á. (eds) *Materials, Technologies and Practice in Historic Heritage Structures*. Springer, Dordrecht (2010). [https://doi.org/10.1007/978-90-481-2684-2\\_13](https://doi.org/10.1007/978-90-481-2684-2_13)
5. Maravelaki-Kalaitzaki, P., Bakolas, A., Moropoulou, A.: Physico-chemical study of cretan ancient mortars, cement and concrete research, vol. 33, no. 5, pp. 651–661 2003. ISSN 0008-8846, [https://doi.org/10.1016/S0008-8846\(02\)01030-X](https://doi.org/10.1016/S0008-8846(02)01030-X)
6. Kapetanaki, K., Kapridaki, C., Maravelaki, P.-N.: Nano-TiO<sub>2</sub> in hydraulic lime-metakaolin mortars for restoration projects: physicochemical and mechanical assessment. *Buildings* **9**, 236 (2019)
7. Maravelaki-Kalaitzaki, P., Karatasios, I., Bakolas, A., Kilikoglou, V.: Hydraulic lime mortars for the restoration of the historic masonry in Crete. *Cem. Concr. Res.* **35**, 1577–1586 (2005)
8. Farmer, V.C.: *Infrared Spectra of Minerals*. Mineralogical Society, London (1974)
9. Maravelaki-Kalaitzaki, P., Agioutantis, Z., Lionakis, E., Stavroulaki, M., Perdikatsis, V.: Physico-chemical and mechanical characterization of hydraulic mortars containing nanotitania for restoration applications (). *Cement Concr. Compos.* **36**(1), 33–41 (2013)
10. Zhu, W., Chen, X., Struble, L.J., Yang, E.H.: Characterization of calcium-containing phases in alkali-activated municipal solid waste incineration bottom ash binder through chemical extraction and deconvoluted Fourier transform infrared spectra. *J. Clean. Prod.* **192**, 782–789 (2018)
11. Moropoulou, A., Bakolas, A., Michailidis, P., Chronopoulos, M., Spanos, C.: Traditional technologies in Crete providing mortars with effective mechanical properties. *Trans. Built Environ.* **15** (1995)